

Complex ac susceptibility studies on a model for granular superferromagnetic CoFe/Al₂O₃

O. Petravic,^{1,2,*} A. Glatz,^{3,4,†} and W. Kleemann²

¹*Physics Department, University of California, San Diego, La Jolla, California 92093*

²*Angewandte Physik, Universität Duisburg-Essen, 47048 Duisburg, Germany*

³*Materials Science Division, Argonne National Laboratory, Argonne, Illinois 60439*

⁴*Institut für Theoretische Physik, Universität zu Köln, 50937 Köln, Germany*

(Dated: February 8, 2020)

Numerical simulations of the magnetization hysteresis and complex ac susceptibility, $\chi = \chi' - i\chi''$, were performed with a model for driven domain walls in random media. We particularly focus on the so-called Cole-Cole plot, χ'' vs. χ' , which can serve as a fingerprint to distinguish different systems by their dynamic behavior. The studies are motivated by recent experimental results on the interacting nanoparticle system [Co₈₀Fe₂₀/Al₂O₃]₁₀ showing superferromagnetic behavior. Its Cole-Cole plot indicates domain wall motion dynamics similarly to a disordered ferromagnet, including pinning and viscous motion. With our model we can successfully reproduce the features found in the experimental Cole-Cole plots.

PACS numbers: 75.60.-d, 75.75.+a, 75.40.Gb, 75.40.Mg

I. INTRODUCTION

The physics of interacting ferromagnetic (FM) nanoparticles is a vivid topic of modern magnetism research. This also applies to the study of the reversal dynamics in thin FM films. The first subject, the properties of interacting FM nanoparticles has been investigated by very many groups focusing either on the preparation (e.g., Ref. 1,2) or the magnetic properties (e.g. Refs. 1,3,4,5,6,7). Numerous theoretical studies were performed in order to understand the observed phenomena or to explore possible new effects (e.g. Refs. 8,9,10,11,12).

While individual single-domain FM nanoparticles exhibit superparamagnetic (SPM) behavior^{1,13,14,15}, interacting ensembles lead to very different kinds of phenomena depending on the type and strength of interactions. Dipolar interactions become relevant since the magnetic moment is of the order $5000\mu_B$, while the distances are of the order 1–10nm. The simple formula for the mean dipolar energy of a particle to one neighbor, $E_{d-d}/k_B = (\mu_0/4\pi k_B)\mu^2/D^3$, yields already 16K for $D = 10$ nm. Considering many neighbors and shorter distances it is obvious, that the effects of dipolar interaction can be observed even at temperatures of the order 100K. In addition, several other types of interactions were proposed, i.e., higher order multipole terms of dipolar^{16,17}, tunneling exchange¹⁸ or even retarded van der Waals interactions¹⁹. Independent from the still open question which interactions are relevant, one can summarize, that essentially three different kinds of phenomena occur:

For large inter-particle distances, and hence a small concentration of particles, the (dipolar) interaction is only a perturbation to the individual particle behavior and no collective behavior is found.^{5,20} For intermediate concentrations a superspin glass (SSG) phase can be found. In this case the particle moments (superspins)

collectively freeze into a spin glass phase below a critical temperature, T_g .^{3,21,22,23} For even higher concentrations a superferromagnetic (SFM) state is encountered. It is characterized by a ferromagnetic arrangement of the moments.^{24,25,26,27} The dynamics resembles at the first glance that of the SSG case, but actually shows features of domain wall motion similar to an impure ferromagnet as will be discussed below.²⁸ Here one should mention that also additional types of collective ordering have been proposed in literature, e.g., the correlated superspin glass state (CSSG).^{29,30}

The second topic, the reversal dynamics in thin ferromagnetic films found equally large interest. Both experimental^{31,32} and theoretical^{31,33,34,35} investigations were performed in order to achieve a better understanding of the processes during the hysteresis cycle. The magnetization reversal occurs either by domain wall (DW) nucleation and motion or by magnetization rotation.³⁶ The DW motion at constant (dc) fields is characterized by three regions depending on the field strength, that is *creep*, *depinning* and *sliding motion*. Creep is the thermally activated motion of DWs, where the average DW velocity is $v(H) \propto \exp[-(U_p/k_B T)(H/H_p)^{-\mu}]$.^{37,38,39} This behavior is encountered at small applied fields, $H \ll H_p$, where H_p is the critical depinning threshold. At zero temperature a dynamic phase transition of second order at $H = H_p$ is found. The mean DW velocity, v , can be interpreted as order parameter of the depinning transition, with $v(H) \propto (H - H_p)^\beta$.⁴⁰ At $T > 0$ the phase transition is smeared out and the $v(H)$ curve is rounded. Beyond the depinning region, $H \gg H_p$, sliding motion sets in and the DW velocity becomes linear with applied field, $v \approx \gamma H$. Here γ is the mobility coefficient.^{41,42}

In alternating (ac) fields, $H = H_0 \sin(\omega t)$, additional dynamical effects will arise. The coercive field and the loop area become dependent on the frequency or in other words on the field sweep rate,^{32,35} dynamic phase transitions and crossovers occur,^{34,41,43} the ac susceptibil-

ity vs. temperature shows similar features as spin glass systems⁴⁴ and a DW velocity hysteresis is found.⁴⁵ Different models have been employed, i.e., numerical solutions of the coupled differential equations of the DW displacement starting from Maxwell's equations³³, using a self-organized "linear" interface depinning model for an elastic DW in random media^{34,41,45} (sometimes referred to as quenched Edwards-Wilkinson⁴⁶ equation), kinetic simulations of a DW in the viscous motion regime³⁵ and calculations based on Fatuzzo's domain theory⁴⁷ applied to ultrathin magnetic layers.³¹

In this paper we will present model investigations motivated by recent experiments on the SFM system $[\text{Co}_{80}\text{Fe}_{20}(1.4 \text{ nm})/\text{Al}_2\text{O}_3(3 \text{ nm})]_{10}$ being a realization of a densely packed ensemble of interacting nanoparticles. The complex ac susceptibility, $\chi' - i\chi''$, reveals that the magnetic dynamic behavior can be explained within the concept of domain wall motion in an impure ferromagnet.^{28,48} That means, the granular system behaves like a thin FM film, only with the difference, that the atomic moments are to be replaced by 'super-moments' of the individual particles. This idea is evidenced from the *Cole-Cole plot*, χ'' vs. χ' .⁴⁹ Hence we will focus on the Cole-Cole presentation and compare it to that found experimentally.

II. COLE-COLE PLOTS

Magnetic systems exhibiting relaxational phenomena can be characterized by the complex ac susceptibility, $\chi(\omega) = \chi' - i\chi''$. One way of presenting the data is the Cole-Cole or Argand representation. The imaginary part is plotted against the real part of the susceptibility, χ'' vs. χ' .^{49,51} It can serve as a fingerprint to distinguish different magnetic systems by their dynamic response. E.g. a monodisperse ensemble of SPM particles has exactly one relaxation time, $\tau = \tau_0 \exp(KV/k_B T)$,^{13,14} and will display a semicircle with the center on the χ' -axis. This can easily be derived from an analytic expression for the ac susceptibility for a monodisperse SPM ensemble with a random distribution of anisotropy axis directions⁸ (Appendix A). In Fig. 1(a) the result is shown for parameters $\mu_0 M_s^2/3K = 1 = KV/k_B T$. In the case of a particle size distribution and hence a distribution of relaxation times the Cole-Cole semicircle is expected to be shifted downward.⁵¹ However, Fig. 1(b) shows two numerically obtained curves, where a particle volume distribution from a log-normal distribution (circles) and a Maxwell distribution⁵⁶ (diamonds) with $\mu_0 M_s^2/3K = 1$, $K/k_B T = 1$, $\tau_0 = 1$, $\Delta V = 0.9$ and $\langle V \rangle = 1$ was assumed. One finds an asymmetric Cole-Cole plot for the case of a log-normal distribution. Obviously this is due to the asymmetry of the distribution itself. By choosing the more symmetric Maxwellian distribution the curve becomes symmetric and also slightly shifted downward. Extremely high polydispersivity is found in spin glass systems, where the distribution of relaxation times is ex-

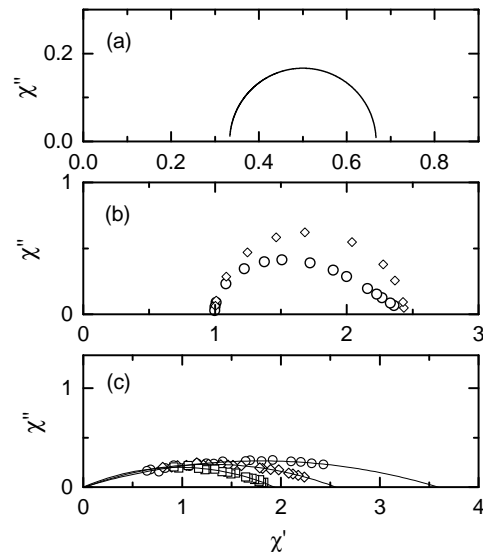


FIG. 1: Cole-Cole plots, χ'' vs. χ' , (a) analytically obtained for a non-interacting monodisperse ensemble of SPM particles with $\mu_0 M_s^2/3K = 1 = KV/k_B T$ (see Appendix A), (b) numerical result for a polydisperse ensemble with a log-normal distribution (circles) and a Maxwell distribution (diamonds) of particle volumes with $\mu_0 M_s^2/3K = 1$, $K/k_B T = 1$, $\tau_0 = 1$, $\Delta V = 0.9$ and $\langle V \rangle = 1$, and (c) shows experimentally obtained curves on the SSG system $[\text{CoFe}(0.9 \text{ nm})/\text{Al}_2\text{O}_3(3 \text{ nm})]_{10}$ at three different temperatures, $T = 50, 55$ and 60 K (Ref. 50).

pected to become infinitely broad⁵². Fig. 1(c) shows an experimentally obtained Cole-Cole plot on the SSG system $[\text{Co}_{80}\text{Fe}_{20}(0.9 \text{ nm})/\text{Al}_2\text{O}_3(3 \text{ nm})]_{10}$ at different temperatures, $T = 50, 55$ and 60 K .⁵⁰

III. MODELS

The time dependent complex ac susceptibility is defined as

$$M(t) = \tilde{\chi}(t)\tilde{H}(t), \quad (1)$$

with the *complex* external field $\tilde{H}(t) = -iH_0 e^{i\omega t}$, ($H(t) = \text{Re}(\tilde{H}(t))$). In this paper we study the time independent term of the Fourier series for $\tilde{\chi}(t)$, namely:

$$\chi \equiv \chi' - i\chi'' = \frac{1}{\mathcal{T}} \int_0^{\mathcal{T}} dt \tilde{\chi}(t), \quad (2)$$

with $\mathcal{T} = 2\pi/\omega = 1/f$.

This defines χ' and χ'' as follows

$$\chi'(\omega) = \frac{1}{H_0 \mathcal{T}} \int_0^\tau dt M(t) \sin(\omega t) \quad (3)$$

$$\chi''(\omega) = -\frac{1}{H_0 \mathcal{T}} \int_0^\tau dt M(t) \cos(\omega t). \quad (4)$$

Or equivalently - if we define $\tilde{\chi}(t) = \frac{dM(t)}{dH(t)} = \dot{M}(t) \left(\frac{dH}{dt} \right)^{-1}$:

$$\chi'(\omega) = \frac{1}{2\pi H_0} \int_0^\tau dt \dot{M}(t) \cos(\omega t) \quad (5)$$

$$\chi''(\omega) = \frac{1}{2\pi H_0} \int_0^\tau dt \dot{M}(t) \sin(\omega t), \quad (6)$$

where $\dot{M}(t) \propto v(t)$, the (mean) DW velocity, which is a function of the external field H and temperature T . We study the complex ac susceptibility in two different approaches:

(i) For the first one, we use the expression for the mean DW velocity in the adiabatic driving regime, given in Ref. 41, which interpolates between the creep regime and sliding DW motion,

$$v(H, T) = \begin{cases} \gamma H F(x, y) & \text{for } H \neq 0, \\ 0 & \text{for } H = 0, \end{cases} \quad (7)$$

where $x = H/H_p$, $y = T_p/T$ and

$$F(x, y) = \frac{\Theta(1-x)}{1 + (yx^{-\mu})^{\beta/\theta}} \exp[yx^{-\mu}(1-x)^\theta] + \Theta(x-1) \left[\frac{1}{1 + (yx^{-\mu})^{\beta/\theta}} + \left(1 - \frac{1}{x}\right)^\beta \right]. \quad (8)$$

Here $\Theta(x)$ is the step function, T_p a typical pinning energy, H_p the depinning field at $T = 0$, γ the mobility coefficient and μ , β and θ the relevant critical exponents⁴¹. The dynamics of the DW is determined by the equation of motion

$$\dot{Z} = v(H(t)), \quad (9)$$

where Z is the (1-dimensional) mean displacement from a flat starting configuration of the DW with $0 \leq Z \leq L_z$ and L_z being the length of the sample in Z -direction. Compared to the experiment this would be a direction in-plane of the sample. Hence the magnetization is

$$M(t) = M_s \left(\frac{2Z(t)}{L_z} - 1 \right). \quad (10)$$

(ii) Since equation (7) was obtained for an adiabatically changing field, it can only be used as an approximation, if the frequency is sufficiently small, $\omega \ll \omega_T(H)$,⁴⁵ (see also Fig. 2 in this Ref.). One should also note, that the above approach does not hold at $T = 0$ and $H < H_p$, since for $\omega > 0$ the depinning transition is smeared out.

In order to include the non-adiabatic effects (e.g., hysteresis of the velocity), one has to start with the underlying equation of motion for a driven d -dimensional interface profile $z(\mathbf{x}, t)$ in a $(d+1)$ -dimensional random medium,⁴⁶ which is also the starting point to obtain Eq. (7):

$$\frac{1}{\gamma} \frac{dz(\mathbf{x}, t)}{dt} = \Gamma \nabla^2 z(\mathbf{x}, t) + H(t) + g(\mathbf{x}, z), \quad (11)$$

where γ and Γ denote the mobility and the stiffness constant of the interface, respectively, and $g(\mathbf{x}, z)$ is the random force with $\langle g \rangle = 0$ and $\langle g(\mathbf{x}, z)g(\mathbf{x}', z') \rangle = \delta^d(\mathbf{x} - \mathbf{x}') \Delta_0(z - z')$, with $\Delta_0(z) = \Delta_0(-z)$ being a monotonically decreasing function which decays over a finite distance ℓ . Here we studied the case $d = 2$. For a detailed study of this equation in the case of an ac driving force in an infinite system see Ref. 45. The mean displacement is $Z(t) = \langle z(\mathbf{x}, t) \rangle_x$ and the mean velocity $v(t) = \dot{Z}(t)$.

Note, that Eq. (11) is written for zero temperature. For finite temperatures an additional thermal noise term $\eta(\mathbf{x}, t)$ has to be added to the r.h.s. of (11). Since the relaxation times for the DW creep at low temperatures are very long ($\gg \omega^{-1}$) and we consider only finite (not exponentially low) frequencies we can concentrate on the zero temperature equation of motion. In Ref. 45 it is shown that thermal effects are not essential for not too low frequencies.

In this paper we will focus on the numerical solution of this equation for finite ($L_z < \infty$) systems. In this case, the DW will hit the boundary of the system for low enough frequencies, such that the magnetization will saturate ($0 \leq M \leq M_s$). Therefore we introduce the critical frequency ω_c or f_c , which depends on L_z , above which the system behaves like an infinite system, i.e., the DW does not reach the system boundary, and below which the magnetization saturates.

For the numerical integration of Eq. (11) it is discretized in x -direction(s) into N^d positions. The disorder $g(\mathbf{x}, z)$ is realized by setting g to random values in $[-1/2, 1/2]$ at positions with distance ℓ . Between these positions g is interpolated linearly which results in a Gaussian $\Delta_0(z)$ with variance ℓ .

IV. RESULTS AND DISCUSSION

Fig. 2 shows an example of hysteresis loops from simulations within approach (i) at $T/T_p = 1.5$ and $H_0/H_p = 1.5$, at different frequencies $f = 0.001$ (a), 0.01 (b), 0.1 (c) and 1.0 Hz (d). The values for the parameters and critical exponents are taken from the literature, i.e., $\gamma = 1.0$,

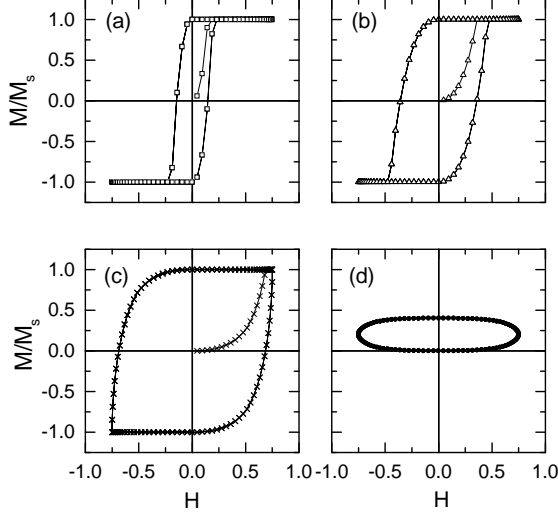


FIG. 2: M/M_s vs. H curves from simulations of a DW in the adiabatic regime with $T/T_p = 1.5$, $H_0/H_p = 1.5$, $\gamma = 1.0$, $\mu = 0.24$, $\theta = 0.83$ and $\beta = 0.66$ at different frequencies $f = 0.001$ (a), 0.01 (b), 0.1 (c) and 1.0 Hz (d).

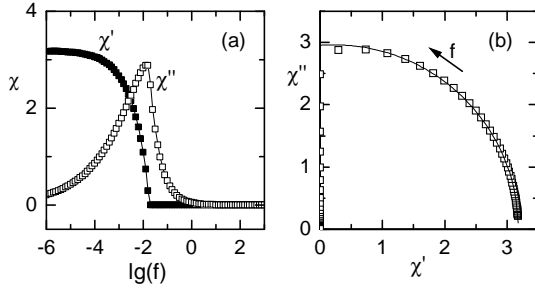


FIG. 3: (a) ac susceptibility, χ' and χ'' vs. ac frequency, f , at $T/T_p = 0.5$, $H_0/H_p = 0.8$ for $\gamma = 1.0$, $\mu = 0.24$, $\theta = 0.83$ and $\beta = 0.66$. (b) Same data, but plotted in the Cole-Cole presentation, χ'' vs. χ' . The solid line represents a least square-fit of the low-frequency data to a circle.

$\mu = 0.24^{39}$, $\theta = 0.83^{53}$ and $\beta = 0.66^{40, 57}$ With increasing frequency the hysteresis loop broadens until it becomes elliptically shaped above $f = 0.1$ Hz losing also its inflection symmetry. Similar results are found in experiments^{28,35}.

The ac susceptibility of such hysteresis cycles can be calculated from equations (3) and (4). In Fig. 3 the obtained data is shown for a specific set of values, $T/T_p = 0.5$ and $H_0/H_p = 0.8$. In (a) one finds the real and imaginary part of the ac susceptibility, χ' and χ'' , as function of the ac frequency. The real part shows an order-parameter like behavior with non-zero value below $f_c = 0.02$, and vanishing value above f_c . However, the imaginary part has a peak around $f_p = 0.016 \approx f_c$.

In the Cole-Cole plot this transition appears as a sharp

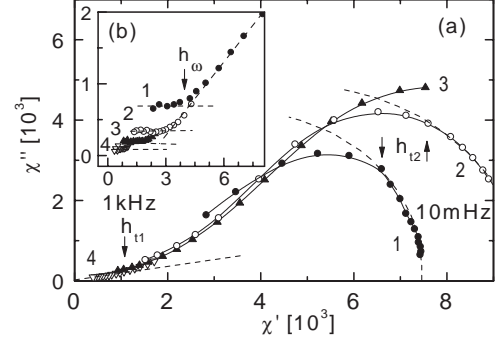


FIG. 4: Experimental Cole-Cole plot taken from Ref. 28 showing χ'' vs. χ' obtained on the SFM granular system $[\text{CoFe}(1.4\text{nm})/\text{Al}_2\text{O}_3(2\text{nm})]_{10}$.

change of the slope and curvature. At low frequencies, $f < f_c$ one observes a quarter-circle centered on the χ' axis (Fig. 3 (b)). This corresponds well to the experimental result^{28,48}(Fig. 4) and suggest the existence of *one* effective relaxation time in the system. However, for $f > f_c$ only a vertical line can be observed. This result differs from that found in experiment, where the high-frequency part is characterized by a concave shape and finite positive slope. This discrepancy needs a closer inspection here.

By comparison of the susceptibility data to the corresponding hysteresis loops, one finds, that $f = f_c$ marks the transition between loops saturating at high fields (low- f) and those, which do not saturate (high- f). In the second case the domain wall is always in motion throughout the entire field cycle. The real part is then zero, whereas the imaginary part has a $1/f$ dependence (Fig. 3 (a)), which follows directly from our result shown in Ref. 28, where the complex susceptibility in the case of viscous DW motion is given by $\tilde{\chi} = \chi_\infty[1 + 1/(i\omega\tau)]$, or more generally by $\tilde{\chi} = \chi'_\infty + \chi''_\infty/(i\omega\tau)$. For $\chi'_\infty = 0$ this yields directly the vertical part in the Cole-Cole plot (Fig. 3 (b)). In Ref. 28 was argued, that the non-linearity of the $v(H)$ function in the creep regime can be taken into account by introducing a polydispersity exponent, β , in the above equation, $\tilde{\chi} = \chi_\infty[1 + 1/(i\omega\tau)^\beta]$ (compare to a similar relationship formulated for the conductivity of disordered hopping conductors $\sigma(\omega) \sim (-i\omega\tau)^{\nu(T)}$, where $0 < \nu < 1$)^{54,55}. This yields the linear relationship, $\chi'' = \tan(\pi\beta/2)[\chi' - \chi_\infty]$. Note, that for *any* velocity function $v = v(H)$ with $v(H) = -v(-H)$ and without velocity hysteresis⁴⁵ it follows, that $\chi' = 0$ and $\chi'' \propto 1/f$. This can easily be seen from Eqs. (5) and (6) and $\dot{M} \propto v$. It means that no linear part can be found in the Cole-Cole plot by considering only the adiabatic motion of one DW.

There are two possible ways to improve the model. The first one is to simulate an ensemble of non-interacting subsystems with different domain wall propagation lengths,

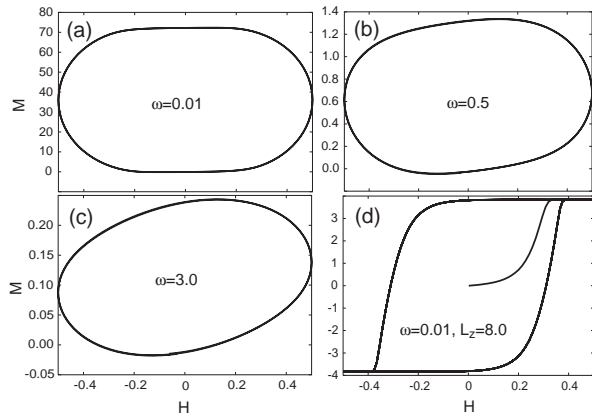


FIG. 5: M vs. H curves from simulations of an EW equation of motion with $H_0 = 0.5$ and different frequencies, $\omega = 0.01$ (a), 0.5 (b) and 3.0 (c) with the DW not touching the boundaries. (d) shows the magnetization curve for $\omega = 0.01$ with the DW touching the boundaries.

pinning fields, H_p or depinning energies, T_p . It is possible, that this case would yield the situation above qualitatively described by the polydispersity exponent $\beta < 1$. The second is to employ a more realistic description of the DW by using the above introduced model (ii). The latter case was studied here.

In Fig. 5 the results for the magnetization hysteresis of a DW from Eq. 11 for $H_0 = 0.5$ are shown ($H_p \approx 0.27$). The plots (a) to (c) show hysteresis loops for different frequencies in the case, when the DW never touches the sample boundary. At low frequencies one finds a symmetric loop with respect to the M axis (a) similar to the result shown above in Fig. 2(d). This symmetry is lost upon increasing the frequency [(b) and (c)] and the loop becomes tilted. This tilting is responsible for a non-vanishing real part of the ac susceptibility and cannot be observed in approach (i). The tilting corresponds to the appearance of a velocity hysteresis.⁴⁵ That means there exists no functional relationship between the velocity and the field any more, as it is the case in the adiabatic regime.

The resulting susceptibilities are plotted in Fig. 6. In (a) and (b) the real and imaginary part vs. $\lg(f)$ and the corresponding Cole-Cole plot, respectively, are shown for an infinite system ($L_z \rightarrow \infty$), when the DW never touches the boundary. In (c) and (d) the same plots are shown for a finite system ($L_z = 8.0$). While the low-frequency parts resemble those from approach (i), the high-frequency part shows a completely different behavior. For $\chi' \rightarrow 0$ we find in the Cole-Cole plot (inset in Fig. 6 (d)) a concave shaped curve similar as in the experiment (Fig. 4). One can expect that χ goes to 0 with $\omega \rightarrow \infty$, since the velocity hysteresis disappears for $\omega \rightarrow \infty$. Obviously the more realistic second model is capable to describe the experimentally found behavior. However, two drawbacks still exist. One, the Cole-Cole plot from the simulation shows a rather steep and nar-

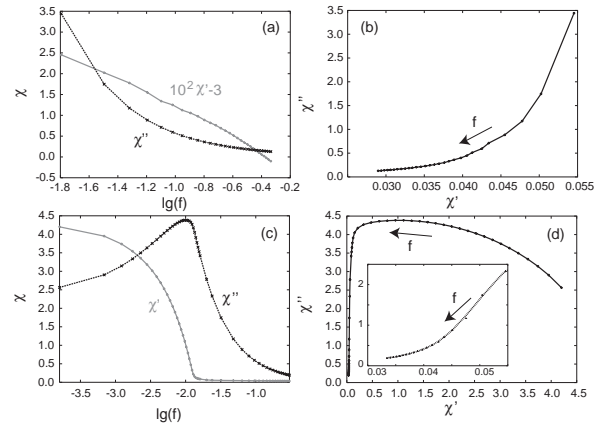


FIG. 6: Real and Imaginary part of the ac susceptibility vs. frequency, calculated with the EW equation of motion (7) for only high frequencies (a) and a wide frequency spectrum (c). All simulations were performed with $H_0 = 0.5$. Plots (b) and (d) are the Cole-Cole plots corresponding to the data shown in (a) and (c), respectively. The inset in (d) shows the high frequency behavior in more detail.

row increasing part compared to the experiment. Second, we cannot retrieve the saturating part for maximum frequencies, where the imaginary part becomes constant (see Fig. 4, inset). This case was attributed²⁸ to the reversible relaxation response of the DW for high frequencies and small excitations fields. It will be interesting to study this case with a suitably modified model which possibly includes multiple and interacting DWs.

V. CONCLUSION

We studied two approaches based on a "linear" interface depinning model in order to get a better understanding of the magnetic behavior found in the superferromagnetic granular multilayer $[\text{Co}_{80}\text{Fe}_{20}(1.4\text{nm})/\text{Al}_2\text{O}_3(3\text{nm})]_{10}$.

Using the first approach with a mean velocity of a domain wall in the adiabatic limit, one can explain the monodisperse dynamic response evidenced by a partial semicircle centered around the χ' axis. However, it fails to describe the increasing concave part for higher frequencies in the Cole-Cole plot. This behavior can be found by taking the full equation of motion into account, where an elastic interface is driven in general *non-adiabatically* in a random medium. Hence a model of an impure ferromagnet is capable to describe the main features of the experimental results. We find that the appearance of a velocity hysteresis is a crucial element in the dynamic response of the superferromagnet. In addition the results confirm, that the above mentioned granular system is neither a superparamagnetic nor a superspin glass system.

Acknowledgments

We thank Ch. Binek and X. Chen for helpful discussions. This work has been supported by the Alexander-von-Humboldt Foundation (O.P.) and the Deutscher Akademischer Austauschdienst (A.G.).

APPENDIX A: THE COLE-COLE PLOT OF A SUPERPARAMAGNETIC SYSTEM

From Ref. 8 one finds an expression for the complex ac susceptibility of a non-interacting monodisperse ensemble of SPM particles in zero-field, where the anisotropy axis directions are randomly distributed.

$$\chi'(\omega) = \mu_0 \frac{M_s^2}{3K} \left[1 + \frac{KV}{k_B T} \frac{1}{1 + (\omega\tau)^2} \right] \quad (\text{A1})$$

$$\chi''(\omega) = \mu_0 \frac{M_s^2}{3} \frac{V}{k_B T} \frac{\omega\tau}{1 + (\omega\tau)^2} \quad (\text{A2})$$

with

$$\tau \approx \tau_0 \exp(KV/k_B T). \quad (\text{A3})$$

Defining $\alpha := \mu_0 M_s^2 / 3K$ and $\sigma := KV/k_B T$ and eliminating ω one gets

$$\chi'' = \sqrt{\left(\frac{\alpha\sigma}{2}\right)^2 - \left(\chi' - \frac{\alpha(2+\sigma)}{2}\right)^2}, \quad (\text{A4})$$

which is a circle with the radius $r = \alpha\sigma/2$ and center at $(\alpha(2+\sigma)/2; 0)$.

-
- * e-mail:opetr@kleemann.uni-duisburg.de
† e-mail:ang@thp.uni-koeln.de
- ¹ J. L. Dormann, D. Fiorani, and E. Tronc, Adv. Chem. Phys. **98**, 283 (1997).
 - ² V. F. Puentes, K. M. Krishnan, and A. P. Alivisatos, Science **291**, 2115 (2001), and References therein.
 - ³ C. Djurberg, P. Svedlindh, P. Nordblad, M. F. Hansen, F. Boedker, and S. Moerup, Phys. Rev. Lett. **79**, 5154 (1997).
 - ⁴ S. I. Woods, J. R. Kirtley, S. Sun, and R. H. Koch, Phys. Rev. Lett. **87**, 137205 (2001).
 - ⁵ F. Luis, F. Petroff, J. M. Torres, L. M. García, J. Bartolomé, J. Carrey, and A. Vaures, Phys. Rev. Lett. **88**, 217205 (2002).
 - ⁶ X. Batlle and A. Labarta, J. Phys. D: Appl. Phys. **35**, R15 (2002).
 - ⁷ S. Sahoo, O. Petravic, W. Kleemann, S. Stappert, G. Dumpich, P. Nordblad, S. Cardoso, and P. P. Freitas, Appl. Phys. Lett. **82**, 4116 (2003).
 - ⁸ J.-O. Andersson, C. Djurberg, T. Jonsson, P. Svedlindh, and P. Nordblad, Phys. Rev. B **56**, 13983 (1997).
 - ⁹ M. Ulrich, J. García-Otero, J. Rivas, and A. Bunde, Phys. Rev. B **67**, 024416 (2003).
 - ¹⁰ P. J. Jensen and G. M. Pastor, New J. Phys. **5**, 68.1 (2003).
 - ¹¹ M. Porto, Eur. Phys. J. B **26**, 229 (2002).
 - ¹² D. Kechrakos and K. N. Trohidou, Phys. Rev. B **58**, 12169 (1998).
 - ¹³ L. Néel, Ann. Geophys. **5**, 99 (1949).
 - ¹⁴ W. F. Brown, Jr, Phys. Rev. **130**, 1677 (1963).
 - ¹⁵ J. L. García-Palacios, Adv. Chem. Phys. **112**, 1 (2000).
 - ¹⁶ P. Politi and M. G. Pini, Phys. Rev. B **66**, 214414 (2002).
 - ¹⁷ V. Russier, J. Appl. Phys. **89**, 1287 (2001).
 - ¹⁸ V. N. Kondratyev and H. O. Lutz, Phys. Rev. Lett. **81**, 4508 (1998).
 - ¹⁹ R. V. Chamberlin, J. Hemberger, A. Loidl, K. D. Humfeld, D. Farrell, S. Yamamuro, Y. Ijiri, and S. A. Majetich, Phys. Rev. B **66**, 172403 (2002).
 - ²⁰ P. E. Jönsson and J. L. García-Palacios, Phys. Rev. B **64**, 174416 (2001).
 - ²¹ J. L. Dormann, D. Fiorani, R. Cherkaoui, E. Tronc, F. Lucari, F. D'Orazio, L. Spinu, M. Nogues, H. Kachkachi, and J. P. Jolivet, J. Magn. Magn. Mater. **203**, 23 (1999).
 - ²² H. Mamiya, I. Nakatani, and T. Furubayashi, Phys. Rev. Lett. **82**, 4332 (1999).
 - ²³ S. Sahoo, O. Petravic, W. Kleemann, P. Nordblad, S. Cardoso, and P. P. Freitas, Phys. Rev. B **67**, 214422 (2003).
 - ²⁴ S. Moerup, M. B. Madsen, J. Franck, J. Villadsen, and C. J. W. Koch, J. Magn. Magn. Mater. **40**, 163 (1983).
 - ²⁵ J. Hauschild, H. J. Elmers, and U. Gradmann, Phys. Rev. B **57**, 677 (1998).
 - ²⁶ M. R. Scheinfein, K. E. Schmidt, K. R. Heim, and G. G. Hembree, Phys. Rev. Lett. **76**, 1541 (1996).
 - ²⁷ W. Kleemann, O. Petravic, Ch. Binek, G. N. Kakazei, Y. G. Pogorelov, J. B. Sousa, S. Cardoso, and P. P. Freitas, Phys. Rev. B **63**, 134423 (2001).
 - ²⁸ X. Chen, O. Sichelschmidt, W. Kleemann, O. Petravic, Ch. Binek, J. B. Sousa, S. Cardoso, and P. P. Freitas, Phys. Rev. Lett. **89**, 137203 (2002).
 - ²⁹ C. Binns, M. J. Maher, Q. A. Pankhurst, D. Kechrakos, and K. N. Trohidou, Phys. Rev. B **66**, 184413 (2002).
 - ³⁰ J. F. Löffler, H.-B. Braun, and W. Wagner, Phys. Rev. Lett. **85**, 1990 (2000).
 - ³¹ B. Raquet, R. Mamy, and J. C. Ousset, Phys. Rev. B **54**, 4128 (1996).
 - ³² W. Y. Lee, B.-C. Choi, Y. B. Xu, and J. A. C. Bland, Phys. Rev. B **60**, 10216 (1999).
 - ³³ H.-T. Wang and S. T. Chui, Phys. Rev. B **60**, 12219 (1999).
 - ³⁴ I. F. Lyuksyutov, T. Nattermann, and V. Pokrovsky, Phys. Rev. B **59**, 4260 (1999).
 - ³⁵ I. Ruiz-Feal, T. A. Moore, L. Lopez-Diaz, and J. A. C. Bland, Phys. Rev. B **65**, 054409 (2002).
 - ³⁶ S. Chikazumi, *Physics of Ferromagnetism Second Edition*

- (Clarendon Press, 1997).
- ³⁷ M. V. Feigelman, V. B. Geshkenbein, A. I. Larkin, and V. M. Vinokur, Phys. Rev. Lett. **63**, 2303 (1989).
 - ³⁸ P. Chauve, T. Giamarchi, and P. Le Doussal, Phys. Rev. B **62**, 6241 (2000).
 - ³⁹ S. Lemerle, J. Ferré, C. Chappert, V. Mathet, T. Giamarchi, and P. Le Doussal, Phys. Rev. Lett. **80**, 849 (1997).
 - ⁴⁰ L. Roters, A. Hucht, S. Lübeck, U. Nowak, and K. D. Usadel, Phys. Rev. E **60**, 5202 (1999).
 - ⁴¹ T. Nattermann, V. Pokrovsky, and V. M. Vinokur, Phys. Rev. Lett. **87**, 197005 (2001).
 - ⁴² R. Cowburn, J. Ferré, S. J. Gray, and J. A. C. Bland, Appl. Phys. Lett. **74**, 1018 (1999).
 - ⁴³ H. Jang, M. J. Grimsen, and C. K. Hall, Phys. Rev. B **67**, 094411 (2003).
 - ⁴⁴ D.-X. Chen, V. Skumryev, and J. M. D. Coey, Phys. Rev. B **53**, 15014 (1996).
 - ⁴⁵ A. Glatz, T. Nattermann, and V. Pokrovsky, Phys. Rev. Lett. **90**, 047201 (2003).
 - ⁴⁶ S. F. Edwards and D. Wilkinson, Proc. R. Soc. London Ser. A **381**, 17 (1982).
 - ⁴⁷ E. Fatuzzo, Phys. Rev. **127**, 1999 (1962).
 - ⁴⁸ O. Petravic, X. Chen, O. Sichelshmidt, Ch. Binek, W. Kleemann, A. Glatz, T. Nattermann, S. Cardoso, and P. P. Freitas, J. Magn. Magn. Mater. (2004), in press.
 - ⁴⁹ K. S. Cole and R. H. Cole, J. Chem. Phys. **9**, 341 (1941).
 - ⁵⁰ O. Petravic, S. Sahoo, Ch. Binek, W. Kleemann, J. B. Sousa, S. Cardoso, and P. P. Freitas, Phase Transit. **76**, 367 (2003).
 - ⁵¹ A. K. Jonscher, *Dielectric Relaxation in Solids* (Chelsea Dielectrics Press, London, 1983).
 - ⁵² J. Mydosh, *Spin Glasses : An Experimental Introduction* (Taylor and Francis, London, 1993).
 - ⁵³ T. Nattermann, Y. Shapir, and I. Vilfan, Phys. Rev. B **42**, 8577 (1990).
 - ⁵⁴ J. Bernasconi, H. Beyeler, and S. Straessler, Phys. Rev. Lett. **42**, 819 (1979).
 - ⁵⁵ T. Ishii, Prog. Theor. Phys. **73**, 1084 (1985).
 - ⁵⁶ In the sense of a Maxwell (velocity) distribution, $(\sqrt{2}V^2/\sqrt{\pi}\Delta V^3) \exp[-V^2/2\Delta V^2]$.
 - ⁵⁷ Note, that the selection of values does not have a significant influence on the behavior under consideration here, especially the qualitative picture does not change.